

SciEn Conference Series: Engineering Vol. 3, 2025, pp 260-264

https://doi.org/10.38032/scse.2025.3.72

Numerical Analysis of Inverted Airfoil for Optimized Aerodynamic Performance in Formula 1

Samin Yaser*, Prasanjit Das

Department of Mechanical Engineering, Chittagong University of Engineering & Technology, Chattogram-4349, Bangladesh

ABSTRACT

The aerodynamics and stability of a vehicle are greatly impacted by its design. A rear wing is an inverted airfoil that provides down-force at high speed. This research seeks to determine the effective airfoil profile & inclination angle of the rear wing in Formula 1, focusing on the computational simulation and analysis of drag and lift coefficients for the NACA 6409, S1223, and FX 63-137 airfoil profiles. Traditional F1 race cars use S1223 as their rear wing. So, we ran simulations on ANSYS Fluent to measure its performance relative to NACA 6409 & FX 63-137 airfoil. In order to keep the simulation realistic, parameters such as airfoil chord length, fluid velocity, density, dynamic viscosity are followed according to standard race conditions to replicate the high-speed environments of Formula 1 racing. The angle of attack ranges from 4° to -12°. The study aims to identify the aerodynamic performance characteristics of each airfoil by comparing their respective drag and lift coefficients. In addition, pressure, velocity & turbulence contours will help us to visualize fluid flow patterns. The results highlight that NACA 6409 generates highest lift to drag ratio of -72.04 at -6° angle of attack. While FX 63-137 produces lift to drag ratio of -70.63 at -4° angle of attack and S1223 gives lift to drag ratio of -67.65 at -4° angle of attack. So, we get an increase of aerodynamic performance of 6.48% for NACA 6409 & 4.4% for FX 63-137 relative to S1223 airfoil. Introducing NACA 6409 in F1 racing will give better results in terms of enhanced aerodynamic performance. This research contributes to the broader understanding of performance optimization in Formula 1 rear wings.

Keywords: Aerodynamics, Airfoil, Angle of Attack, Lift to Drag Ratio.



Copyright @ All authors

This work is licensed under a Creative Commons Attribution 4.0 International License.

1. Introduction

Downforce is an aerodynamic force that pulls the body of a vehicle down towards the track, improving its grip and stability in high-speed. Spoilers such as inverted airfoils are used in F1 vehicles to overcome excessive lift force generated due to the pressure differential at higher speeds. Numerous studies have explored airfoil simulations and the aerodynamic performance of F1 cars. However, there is a noticeable lack of research dedicated to airfoil simulations specifically tailored for F1 vehicles. This underscores the necessity for a comprehensive analysis of airfoil performance in the context of F1 applications, where optimizing aerodynamics is essential. This study conducts a comprehensive performance analysis of three airfoils S1223, NACA 6409, and FX 63-137. S1223 airfoil, a wellestablished traditional design, serves as the benchmark for comparison. By analyzing the aerodynamic properties of NACA 6409 and FX 63-137 relative to S1223, the study seeks to identify potential performance advantages and limitations of alternative airfoil designs under similar operational constraints. Md Mahfujul Islam and Mohammad Ilias Inam performed numerical investigation of the effect of different airfoil profile of a spoiler in a car. Despite the fact that spoilers minimize lift, they actually, increase drag, as seen in this research. Drag force is increased by 14% by

attaching spoiler [1]. Mustafa Cakir conducted CFD simulations for aerodynamic effects of a rear wing on a passenger vehicle. While using wings both C_D and C_L (negative lift) decreases. Aerodynamic drag is reduced by

17% and 7% lift is reduced. On the other hand, the drag slightly increases while using spoiler [2].

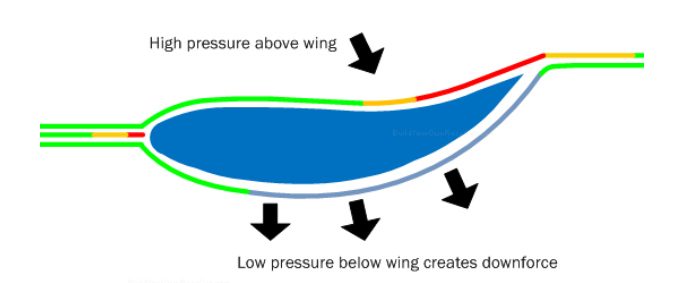


Fig. 1. Generating downforce from spoiler [3]

Mohamed Adel El Hady performed a comparative study for three different airfoils NACA 0012, NACA 2412, and SG6043. It is observed that SG6043 profile has the highest value of lift to drag ratio [4]. Mahmoud Ibrahim Youssef used CFD analysis to investigate the appropriate height of the rear spoiler on a car. It's found that the installation of a spoiler at the height of 371mm upper surface of the vehicle

trunk, the total drag coefficient reduction of 26% [5]. A R S Azmi, A Sapit, A N Mohammed, M A Razali, A Sadikin, N Nordin studied airflow characteristics of rear wing of F1 car. NACA 2408, NACA 2412, NACA 2415 was used for this. Wing flaps gap were 10mm and 50mm. NACA 2415 with short flap wing has the highest L/D for both gap of 10mm and 50mm [6].

2. Methodology

2.1 Governing Equation

Continuity equation for 2D, incompressible, steady state flow

$$\frac{\partial u}{\partial x} + \frac{\partial v}{\partial y} = 0 \tag{1}$$

For 2D, incompressible, steady state flow the Navier Stokes [7] equation is

$$\rho \left(u \frac{\partial u}{\partial x} + v \frac{\partial u}{\partial y} \right) = -\frac{\partial p}{\partial x} + \mu \left[\frac{\partial}{\partial x} \left(\frac{\partial u}{\partial x} \right) + \frac{\partial}{\partial y} \left(\frac{\partial u}{\partial y} \right) \right] + \rho g_x$$
 (2)

$$\rho \left(u \frac{\partial v}{\partial x} + v \frac{\partial v}{\partial y} \right) = -\frac{\partial p}{\partial y} + \mu \left[\frac{\partial}{\partial x} \left(\frac{\partial v}{\partial x} \right) + \frac{\partial}{\partial y} \left(\frac{\partial v}{\partial y} \right) \right] + \rho g_y$$
 (3)

Transport equation of SST k-ω model [8]

$$\frac{\partial}{\partial t}(\rho k) + \frac{\partial y}{\partial x i j}(\rho k u i) = \frac{\partial}{\partial x j}\left(\Gamma k \frac{\partial k}{\partial x i}\right) + Gk - Yk + Sk \qquad (4)$$

$$\frac{\partial}{\partial t}(\rho w) + \frac{\partial y}{\partial xij}(\rho wuj) = \frac{\partial}{\partial xj}\left(\Gamma w \frac{\partial w}{\partial xj}\right) + Gw - Yw + Sw (5)$$

In Eq. (4), the term G_k represents the production of turbulence kinetic energy. In Eq. (5) G_{ω} represents the generation of ω . Γ_k and Γ_{ω} represent the effective diffusivity of k and ω respectively. Y_K and Y_{ω} represents the dissipation of k and ω due to turbulence. D_{ω} represents the cross-diffusion term. S_K & S_W are user defined source term. In Eq.(1) and (2) u & v denotes the velocity in a specified direction.

2.2 Geometry and Mesh

Airfoil profiles used for simulation are NACA 6409, Selig 1223, FX 63-137. These airfoil profiles are plotted in ANSYS SpaceClaim. The coordinates are imported from UIUC Data Site. The chord length of the airfoil is 250mm. We have taken C type fluid domain in consideration. For the fluid domain, the semicircle radius is 1875mm and the dimension of the square is 3750mm x 3750mm.

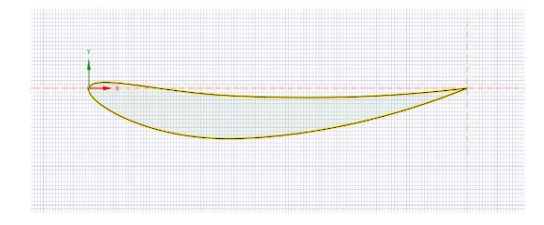


Fig.2. NACA 6409 geometry

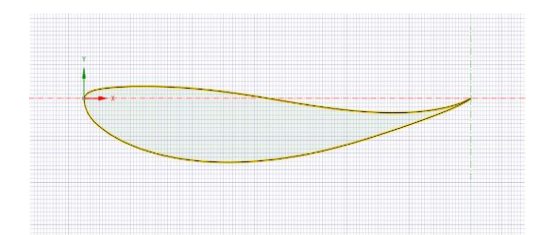


Fig. 3. FX 63-137 geometry

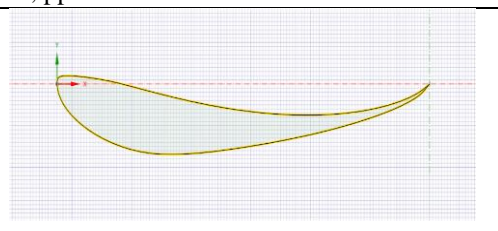


Fig. 4. S1223 geometry

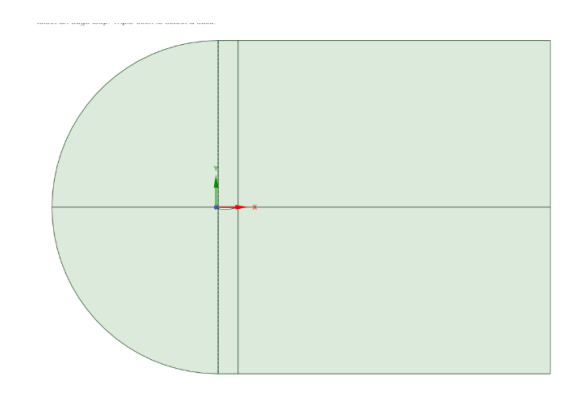


Fig. 5. C type fluid domain surface

The fluid domain and the airfoil were divided into 6 parts and the edges were divided into number of divisions and along with the biasing factor. C type mesh is used for better convergence. The mesh contains 200900 nodes and 200000 elements.

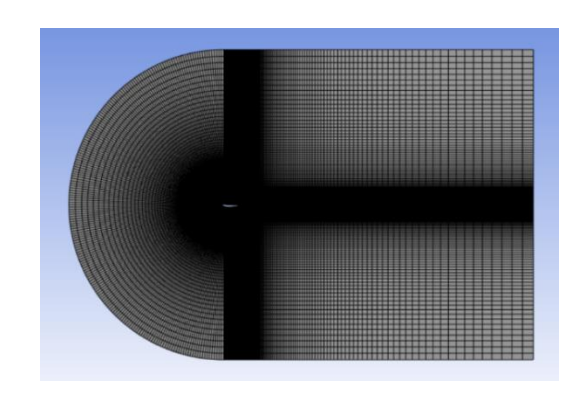


Fig. 6. Mesh of fluid domain

2.3 Solver Settings

Table 1. Solver setting in the ANSYS

Table 1. Solver setting in the ANS 15	
Solver	Steady state, 2D Pressure based
Turbulence model	Viscous k-omega SST
Materials	Fluid: Air
	Solid: Aluminum
Velocity specification	Components
Velocity inlet	83.3 m/s
Gauge pressure	0 Pa
Residuals	1x10 ⁻⁶
Reference Values	Temperature: 288.16 K
	Density: 1.225 kg/m ³
	Viscosity: 1.81x10 ⁻⁵ kg/ms
	Area: 0.25 m ²

Table 1 shows the overall setting for the simulation. Turbulence model k-omega is used for the simulation. Velocity is approximately 300 km/h (83.3 m/s). Velocity is divided into X & Y components for variable angle of attack. Properties such as temperature, density, viscosity etc. are taken at 15°C as standard racetrack temperature is close to 15°C. We have performed 1000 iterations for convergence.

3. Result and Discussion

3.1 Discussion of Various Contour

This study involves generating pressure, velocity and turbulence contours to observe flow characteristics around the airfoil. These results provide insights into effects of airflow on the airfoil's behavior under different conditions.

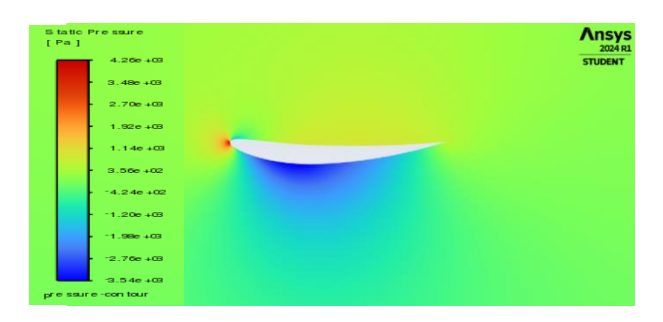


Fig. 7. NACA 6409 pressure contour

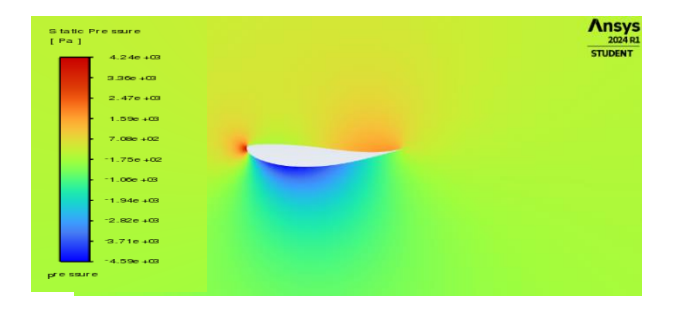


Fig. 8. FX 63-137 pressure contour

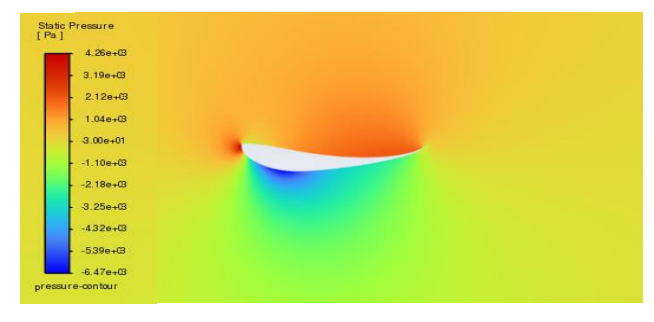


Fig. 9. S1223 pressure contour

From fig.7,8,9 we see, the region at top of the airfoils indicates higher pressure than the bottom of the airfoil. This indicates that the lift is negative which means that the airfoils are inducing downforce. Also, we can see that, at the leading edge the pressure is highest which signifies the stagnation point. Also, we see the variation of the pressure contours for different airfoils.



Fig. 10. NACA 6409 velocity contour



Fig. 11. FX 63-137 velocity contour



Fig. 12. S1223 velocity contour

From the fig.10,11,12 we see that the region below the airfoil has higher velocity than the top of the airfoil surface. From Bernoulli's principle, we know that low velocity airflow induces higher pressure and vice versa. So, it is evident that the airfoils are producing downforce. Also, we can see the stagnation point at the leading edge due to zero velocity.

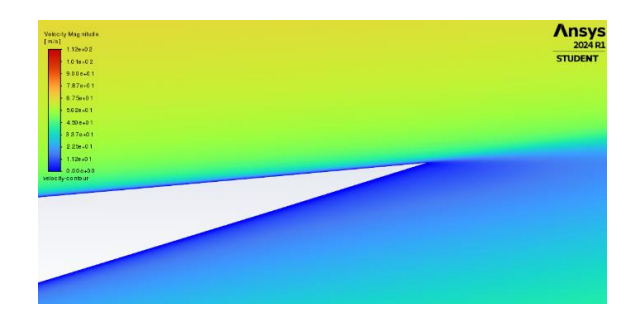


Fig. 13. Closeup view of the trailing edge

From fig.13 we get to look at the trailing edge of the airfoil. Due to no-slip condition, we can see that velocity along the airfoil surface is zero.

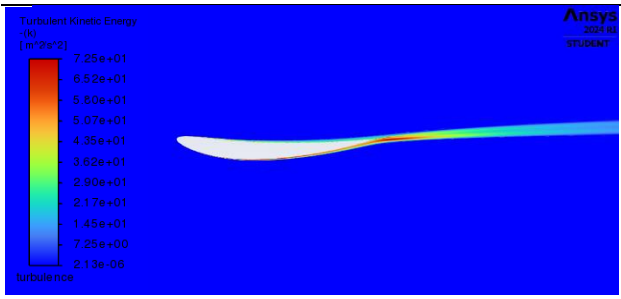


Fig. 14. NACA 6409 turbulence contour

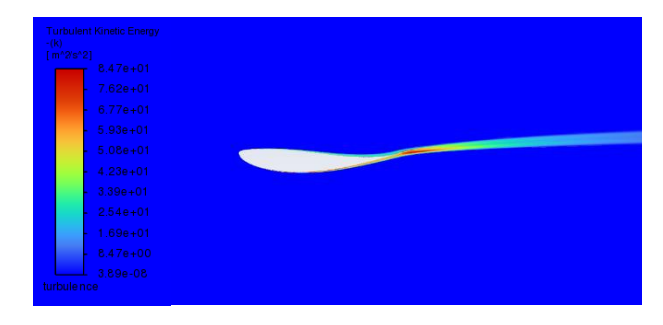


Fig. 15. FX 63-137 turbulence contour

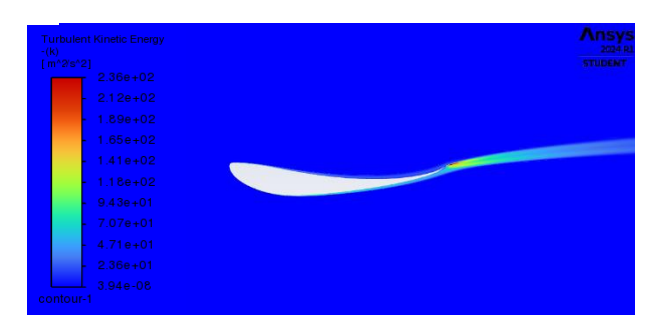


Fig. 16. S1223 turbulence contour

From fig.14,15,16 we can see that, turbulence occurs at the trailing edge of the airfoil. It is due to the separation of flow at the trailing edge. Due to this phenomena, eddies form behind the trailing edge which causes turbulence.

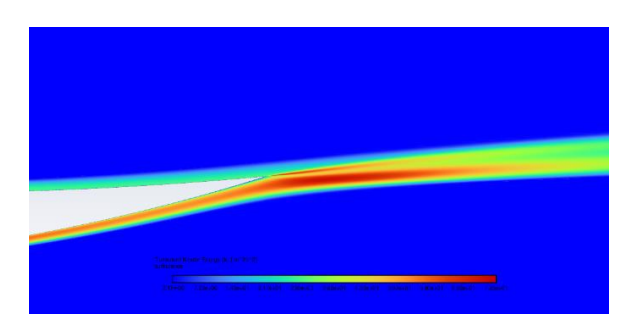


Fig. 17. Closeup view at the turbulence zone

From fig.17 we see how the turbulence corresponds to separation of the airfoil. We can see high amount of turbulence indicating the red zone at the trailing edge of the airfoil. Flow separation results in formation of eddies.

3.2 Graphical Representation of Obtained Result

We ran the simulations for every airfoils where the angle of attack ranged from 4° to -12°. The results obtained from the simulation are accumulated in the following graphs.

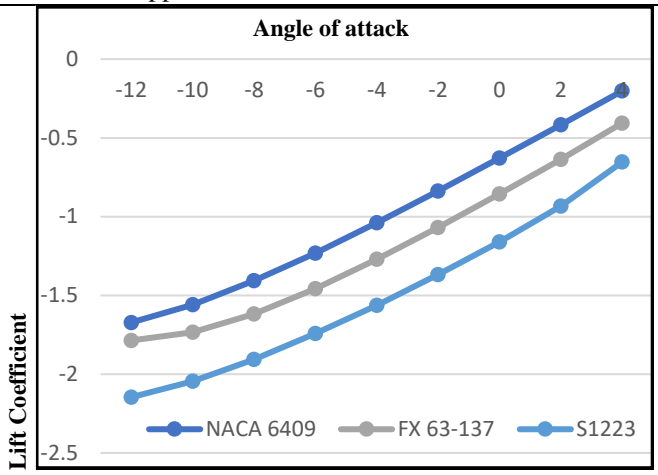
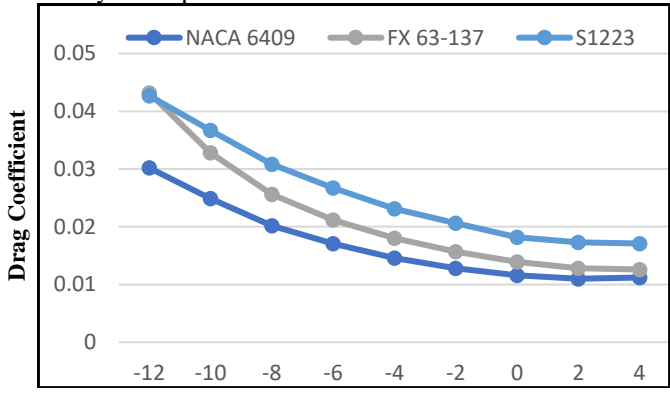


Fig. 18 angle of attack \propto vs lift coefficient C_L

From fig.18 we clearly see that as the angle of attack increases, the lift coefficient increases. The negative value of lift indicates the downforce. From the graph, we see that S1223 shows better downforce than the other two airfoils. In terms of downforce, FX 63-137 airfoil comes after S1223. But the NACA 6409 airfoil shows least downforce than the other two airfoils. Higher downforce gives better aerodynamic performance.



Angle of attack Fig. 19. angle of attack \propto vs drag coefficient C_D

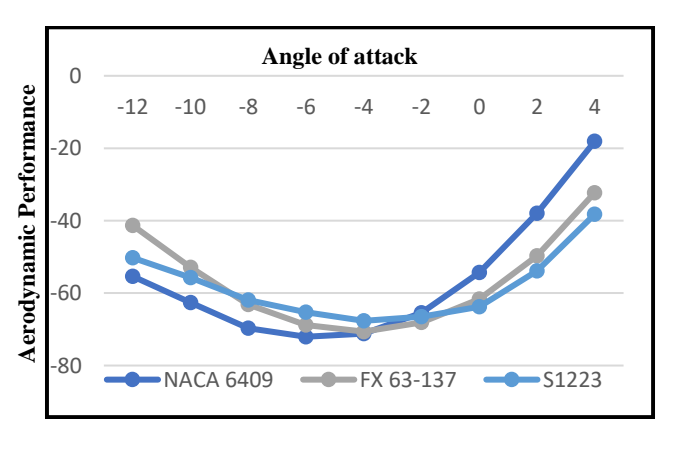


Fig. 20. angle of attack \propto vs C_L/C_D

From fig.19 we see that the drag coefficients drop as the angle of attack increases. We see that NACA 6409 airfoil shows the least amount of drag & S1223 shows the most amount of drag. Less drag is beneficial for high-speed straights.

From fig.20 we see that the C_L/C_D decreases first and then it increases with the increment of alpha. The most amount

of C_L/C_D approaches at -6° to -2°. The NACA 6409 airfoil shows the highest C_L/C_D of -72.04 at -6°. The FX 63-137 gives a closer value of -70.63 at -4°. While S1223 gives highest C_L/C_D of -67.65 at -4°.

4. Validation

In the absence of previous research for direct validation, the accuracy of the simulation is verified by adhering to a suitable y+ value. Ensuring the y+ value remains within the optimal range for capturing the near-wall region in CFD simulations affirms the reliability of the aerodynamic results obtained in this study. The y+ value in CFD is a nondimensional metric that measures the spacing between the wall and the first computational node, scaled by the local viscous length. This parameter is essential for evaluating the adequacy of mesh refinement in resolving turbulence, particularly in capturing the near-wall flow dynamics, interactions within including the viscous sublayer or buffer zone.

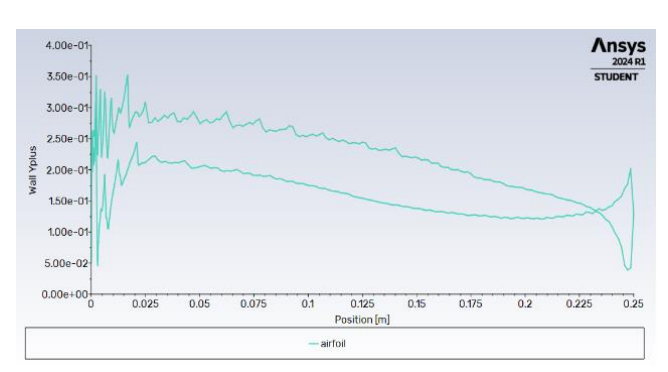


Fig. 21. Wall y+ value along the airfoil surface

From fig.21 we see that the maximum value of y+ is 0.35 which is well below 1. At y+ value of 0.35, the initial grid point is positioned deep inside the viscous sublayer, where viscous forces are predominant and turbulent disturbances are minimal. This configuration implies an exceptionally refined mesh in the proximity of the wall, allowing for an accurate depiction of flow dynamics without resorting to wall function methods.

5. Conclusion

In summary, this research provides a comparative evaluation of the aerodynamic performance for the NACA 6409, FX 63-137, and S1223 airfoils at various angles of attack, specifically for Formula 1 applications. Among the tested airfoils, the NACA 6409 exhibited superior aerodynamic performance. NACA 6409 has the best C_L/C_D of -72.04 at -6°. While FX 63-137 produces C_L/C_D of -67.65 at -4°. In general, S1223 exhibited better downforce than other airfoils while NACA 6409 exhibited lower drag than other airfoils. The results suggest that we get an increase of aerodynamic performance of 6.48% for NACA 6409 & 4.4% for FX 63-137 relative to S1223. This performance highlights its potential for Formula 1 vehicles, where optimizing the elift-

to-drag ratio is crucial for maximizing speed and stability. The results suggest that the NACA 6409 is particularly suitable for Formula 1, where high aerodynamic efficiency is vital.

References

- [1] M. I. I. Md.Mahfujul Islam, "Numerical Investigation of the effect of different Aerofoil profile of a spoiler in a car," in *International Conference on Mechanical, Industrial and Energy Engineering* 2022, 2022.
- [2] M. Cakir, "CFD study on aerodynamic effects of a rear wing," 2012.
- [3] "Build Your Own Race Car," [Online]. Available: https://www.buildyourownracecar.com/race-car-aerodynamics-basics-and-design/4/. (23 October 2024)
- [4] M. A. E. Hady, "A comparative study for different shapes of airfoil," *Journal of Advanced Research in Fluid Mechanics and Thermal Sciences*, vol. 69, no. 1, pp. 34-45, 2020.
- [5] M. I. Y. M. Youssef, "Using CFD Analysis to Investigate the Appropriate Height of the Rear Spoiler on a Car," *International Journal of Mathematics and Physical Sciences Research*, vol. 10, pp. 38-44, 2022.
- [6] A. S. A. N. M. M. A. R. A. S. N. N. A. R. S. Azmi, "Study on airflow characteristics of rear wing of F1 car," in *IOP Conference Series: Materials Science and Engineering, Institute of Physics Publishing*, 2017.
- [7] "Cadence," [Online]. Available: https://resources.system-analysis.cadence.com/blog/msa2022-formulating-the-2d-incompressible-steady-state-navier-stokes-equation. (23 October, 2024)
- [8] "SLIMSCALE," [Online]. Available: https://www.simscale.com/docs/simulation-setup/global-settings/k-omega-sst/. (23 October, 2024)

NOMENCLATURE

C_D: Coefficient of Drag.

C_L: Coefficient of Lift.

 C_L/C_D : Lift to drag ratio/Aerodynamic Performance.

∝ : Angle of attack

y+: A non-dimensional metric that measures the spacing between the wall and the first node.